REPORT DOCUMENTATION PAGE

AFRL-SR-AR-TR-08-0022

1. REPORT DATE (DD-MM-YYYY)	2. REPORT TYPE	3. DATES COVERED (From - To)
	Final Technical Report	1 December 2003 – 31 May 2007

4. TITLE AND SUBTITLE
Microstructure Evolution and Mechanical Properties of Severely Plastically Deformed (SPD) Aluminum Alloys

5a. CONTRACT NUMBER

5b. GRANT NUMBER
FA9550-04-1-0018

5c. PROGRAM ELEMENT NUMBER

6. AUTHOR(S)
Dr. Surya R. Kalidindi

5d. PROJECT NUMBER

5e. TASK NUMBER

5f. WORK UNIT NUMBER

7. PERFORMING ORGANIZATION NAME(S) AND ADDRESS(ES
Department of Materials Science and Engineering
Drexel University
3201 Arch Street, Suite 100
Philadelphia PA 19104

8. PERFORMING ORGANIZATION REPORT NUMBER

9. SPONSORING/MONITORING AGENCY NAME(S) AND ADDRESS(ES)
USAF/AFRL
AFOSR
875 North Randolph Street
Arlington VA 22203
Brett Conner/NA

10. SPONSOR/MONITOR'S ACRONYM(S)
AFOSR

11. SPONSORING/MONITORING AGENCY REPORT NUMBER
N/A

12. DISTRIBUTION AVAILABILITY STATEMENT

Distribution Statement A: Approved for public release. Distribution is unlimited.

13. SUPPLEMENTARY NOTES

14. ABSTRACT
A combined experimental and modeling study has been carried out to characterize the structure and mechanical properties of severely plastically deformed (SPD) aluminum and its alloys as well as the effect of strengthening mechanism on fracture toughness and failure mode. This investigation is focused specifically on Equal Channel Angular Pressing (ECAP) and heavy cold rolling of high solute Al alloys. A particular reason for studying the high strength potentially achievable by these routes is the expectation that since the fracture toughness of precipitation hardened aluminum alloys is known to be degraded by grain boundary precipitates, the high strengths achievable by strain hardening without precipitation has a reasonable prospect of yielding a higher combination of yield strength and toughness than by conventional precipitation hardening. In this study it has been shown that that SPD processing of high solute Al alloys can be carried out to higher strains before strain localization occurs if mechanical stress relieving is done prior to processing and that strengths unobtainable through precipitation hardening can readily be achieved by strain hardening. The effect of natural aging on strain hardening has been investigated and found to be a significant factor in the rate at which the flow stress increases with increasing plastic strain. It has been shown that strain hardened Al alloys are more ductile and exhibit higher strain hardening rates then precipitation hardened alloys at equivalent strengths and that strain hardening is a viable processing route for improving toughness. On the modeling side, we have developed new micromechanical finite element models that employ crystal plasticity constitutive framework and are able to successfully simulate texture evolution in the sample during complex routes of ECAP.

15. SUBJECT TERMS

MICROSTRUCTURE EVOLUTION AND MECHANICAL PROPERTIES OF SEVERELY PLASTICALLY DEFORMED (SPD) ALUMINUM ALLOYS

FA9550-04-1-0018

Surya R. Kalidindi, Roger D. Doherty,
Christopher J. Hovanec, Brendon R. Donohue, and Ryan J. VanderMeulen
Department of Materials Science and Engineering
Drexel University, Philadelphia

Abstract

A combined experimental and modeling study has been carried out to characterize the structure and mechanical properties of severely plastically deformed (SPD) aluminum and its alloys as well as the effect of strengthening mechanism on fracture toughness and failure mode. This investigation is focused specifically on Equal Channel Angular Pressing (ECAP) and heavy cold rolling of high solute Al alloys. A particular reason for studying the high strength potentially achievable by these routes is the expectation that since the fracture toughness of precipitation hardened aluminum alloys is known to be degraded by grain boundary precipitates, the high strengths achievable by strain hardening without precipitation has a reasonable prospect of yielding a higher combination of yield strength and toughness than by conventional precipitation hardening. In this study it has been shown that that SPD processing of high solute Al alloys can be carried out to higher strains before strain localization occurs if mechanical stress relieving is done prior to processing and that strengths unobtainable through precipitation hardening can readily be achieved by strain hardening. The effect of natural aging on strain hardening has been investigated and found to be a significant factor in the rate at which the flow stress increases with increasing plastic strain. It has been shown that strain hardened Al alloys are more ductile and exhibit higher strain hardening rates then precipitation hardened alloys at equivalent strengths and that strain hardening is a viable processing route for improving toughness. On the modeling side, we have developed new micromechanical finite element models that employ crystal plasticity constitutive framework and are able to successfully simulate texture evolution in the sample during complex routes of ECAP.

1. Background

The two most potent methods of strengthening aluminum, as well as other metals, are strain hardening and precipitation hardening. Precipitation hardening has, since its discovery one hundred years ago, been the dominant strengthening method for Al alloys for two apparent reasons. Firstly, its processing convenience – thick, irregularly-shaped pieces can be precipitation treated almost as effectively as thin, regular ones. Secondly, aluminum has a large stacking fault energy which allows for dynamic recovery to easily occur, resulting in ineffective work hardening at room temperature. However, the realization that solute can greatly enhance the resistance to dynamic recovery in aluminum alloys and thus give very potent strain hardening was exploited successfully by the beverage can industry (see for example [1]). Additionally, previous studies [2] & [3] have demonstrated that very high strengths can be achieved by conventional rolling of high solute solution treated alloys such as Al-Mg-Si, Al-Mg-Cu and Al-Zn-Mg-Cu. This is a significant finding from an engineering standpoint due to the development of novel processing techniques, such as ECAP, which is capable of imposing large stains [4], while retaining a cross sectional area capable of being used in load bearing applications. Finally, recent work by the authors and their students [5] has suggested that it might be possible to significantly increase the toughness of high strength aluminum alloys if grain boundary precipitation could be avoided. Strengthening by strain hardening high solute alloys will avoid the precipitation step that inevitably produces embrittling grain boundary precipitates [6]. In other words, strengthening by strain hardening may allow higher combinations of strength and toughness in Al alloys.

2. Work and Accomplishments

The work carried out in this study was an integrated combination of experiments and modeling. This section will detail the work and accomplishments in each area. For clarity, this section has been subdivided to two sections, one of which deals primarily with the experimental effort and the second with the modeling effort.

2.1 Experimental Work and Accomplishments

Investigation of the Role of Solute on Work Hardening Rates in Al alloys: Detailed experiments were designed and carried out to better understand the underlying physics of strain hardening in high solute Al alloys [7, 8]. The studies were aimed at answering the following questions: 1) Is strain hardening more effective with solute in solution or precipitated as GP zones? 2) What is the effect of a high dislocation density on the formation of GP zones?

In order to answer the above questions, a series of deformation (cold rolling) experiments, after different periods of natural aging, were carried out on a 2xxx series (4.5 wt% Cu, 1.5 wt% Mg, 0.5 wt% Mn) aluminum alloy that would both effectively strain harden and naturally age. The microstructural changes were indirectly monitored by eddy current electrical conductivity and Rockwell B hardness measurements as a function of time after quenching. The full details of the experimental procedure are described in [7, 8]. The hardening increments due to GP zone formation and strain hardening, as well as the associated drop in electrical conductivity are shown in Figure 1.

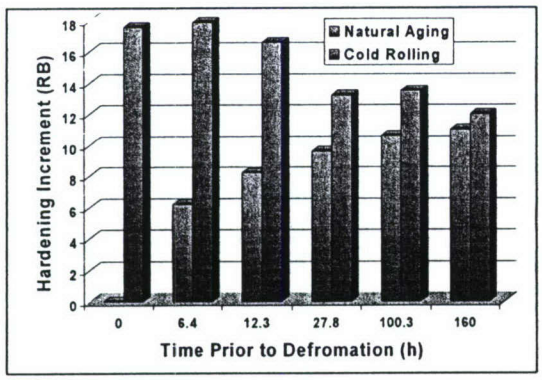

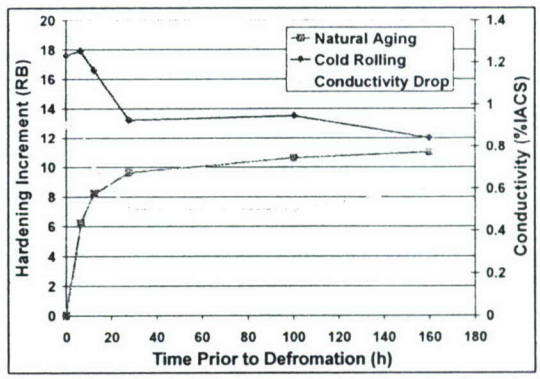

Figure 1: (a, left) Increment of hardening due to natural aging for different time periods and subsequent cold rolling after aging. (b, right) Increment of hardening (right axes) and electrical conductivity drop (left axes) plotted against time at deformation [7, 8].

Regardless of what point during the aging process the samples were rolled each showed an increase in hardness, as a result of the deformation, and no additional hardening due to continued aging. Not only was there no age hardening, but the other characteristic of GP zone formation, a fall in electrical conductivity with time, was not seen. It is known that the natural aging process, in the 2xxx alloys, stops when the excess vacancies produced by quenching are lost and the diffusion coefficient returns to the very low value expected at room temperature, effectively stopping the formation of GP zones [9]. At room temperature the bulk diffusion rate of solute in Al is so small that the time frame for GP zones to form would be orders of magnitude larger then the 3 to 4 days observed. By introducing a large dislocation density into the microstructure that acts as a sink for vacancies it is possible to inhibit natural aging and stop the formation of GP zones.

As time before rolling increased and more GP zones formed, the increment of hardening due to aging increased but the increment of strain hardening decreased, as shown in Figure 1a. As time prior to cold rolling increases there is a reduction in the effectiveness of strain hardening in the presence of GP zones. The drop in electrical conductivity upon cold rolling was attributed to the increase in dislocation density, and it can be seen in Figure 1b that the drop in conductivity decreases with the formation of GP zones. This reinforces the observation that the alloy more effectively strain hardened before the solute forms GP zones. The decrease in the magnitude of conductivity drop can be attributed to more dynamic recovery, resulting in less of a strain hardening increment. By plotting the hardness and conductivity data together, the relationship between the increment of strain hardening and drop in electrical conductivity is more easily seen, as shown in Figure 1b. The most striking feature in Figure 1b is the similarity in the profiles of the strain hardening curve and the drop in electrical conductivity curve. This also supports the theory that dynamic recovery is more effectively inhibited by solute in solution than GP zones. It should be noted that this experiment was also performed at a rolling strain of 0.1 and the dislocation density was insufficient to totally inhibit natural aging, although the natural hardening increment was reduced to approximately 15% of a fully aged increment of hardening. Further details of this study are presented in [7, 8].

Solute Enhanced Strain Hardening of Aluminum Alloys: Strain hardening, one of the oldest and most widely exploited strengthening mechanisms of metals, is largely ignored in aluminum based alloys. The reason for this is that aluminum alloys have a high stacking fault energy (SFE). Due to this high SFE the dislocations that are produced during plastic deformation are not as readily retained (dynamic recovery) as they are in other alloys. This has led the field to design alloys to effectively precipitation harden. It was later discovered that these solute rich alloys designed for artificial aging exhibited higher strain hardening rates than anticipated, provided that the solute is kept in solution (T4 or W temper). This discovery has prompted the investigation of strain hardening and *solute enhanced strain hardening* of aluminum alloys.

Through the use of industrial and novel deformation methods (cold rolling, pressing, ECAP) yield strengths previously unachievable in aluminum alloys have been realized. Complete details of the processing are given in [10, 11]. Commercial purity Al, processed to a true strain of 10 exhibits a yield strength of 180MPa, which is six times stronger than in the annealed condition (30MPa), as show in Figure 2.

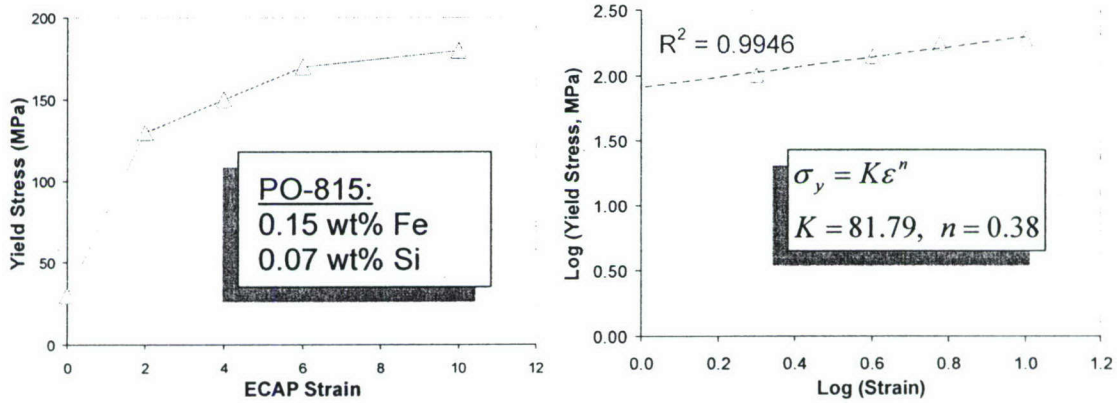

Figure 2. (a) Yield strength plotted against ECAP processed strain and (b) the corresponding Hollomon-Stump relationship for commercial purity Al.

More impressively alloy 2524 exhibits yield strengths as high as 620MPa at much lower strains (the highest yield strength that can be produced by precipitation hardening, T6-temper, in this alloy is 430MPa). The level of strain required to produce strengths in this alloy that are comparable to those achieved by precipitation hardening can easily be imposed on an industrial scale. The non-heat treatable alloy 5182 also showed a significant increase in strength compared to its annealed condition, as shown in Table 1 and Figure 3a.

Alloy	Yield Strength (MPa)		
	Annealed	Peak aged	ECAPed
P0-815	30	--	130
5182	135	--	400
2524	240	430	620

Table 1: Yield strengths of Al alloys with increasing amounts of solute in various processing conditions.

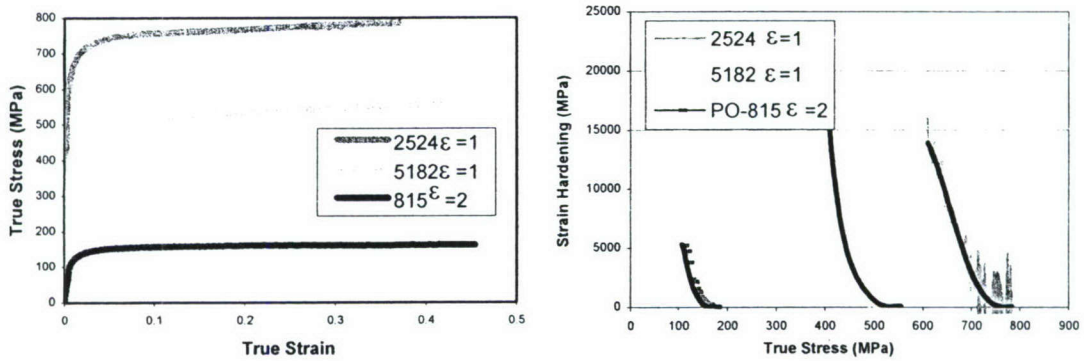

Figure 3. (a) True stress-true strain plots produced by compression testing post-processed Al alloys of various solute levels and (b) the corresponding strain hardening rate.

Examination of the mechanical response of the strain hardened material not only depicts the impressive increase in strength but also reveals the previously reported trend that as the amount of solute in solution increases so does the strain hardening rate, as shown in Figure 3b. It should be noted that as the level of strain is increased during processing, the strain hardening rate decreases and failure by strain localization eventually occurs (this is not a new insight and occurs and all alloy systems).

The Influence of Deformation History and Texture on the Hall-Petch Relationship: The Hall-Petch relationship, correlating a metal's grain size to its yield strength, has been known about and exploited in both ferrous and non-ferrous alloys for over 50 years now, most successfully in the steel industry. However, Aluminum alloys are not strongly affected by this grain size-yield strength relationship and the reasons for this remain largely unknown. Furthermore, the reported Hall-Petch values for aluminum have been known to contain large amounts of scatter and do not take into account what effects texture may have on the relationship. It is widely known that crystallographic texture plays a significant roll in the properties of polycrystalline metals.

This part of the study began with two core questions to be addressed. The first being what effect do LAGB have on the Hall-Petch relationship and secondly does texture have a significant affect on it. It may be possible that these unaccounted for variable are practically responsible for the variation in the literature. To explore these questions a commercial purely aluminum alloy was selected (PO-815) and thermomechanically processed by two different routes. This was done to create samples with different crystallographic textures but with overlapping grain sizes. The full details of the processing procedure are described in [12, 13]. One batch of material was cold rolled to increasing amounts of strain and recrystallized in the typical discontinuous Gibb's type I transformation to produce material with decreasing grain sizes and increasing yield strengths. A second batch of material was ECAP processed to produce SPD structures which when exposed to annealing temperatures coarsen in a continuous Gibb's type II transformation retaining the deformation texture. The Hall-Petch plot for this data is shown in Figure 4. The difference in yield strength and K_y values at similar grain sizes is apparent, although, there is good agreement in the frictional flow stress values (~26 MPa).

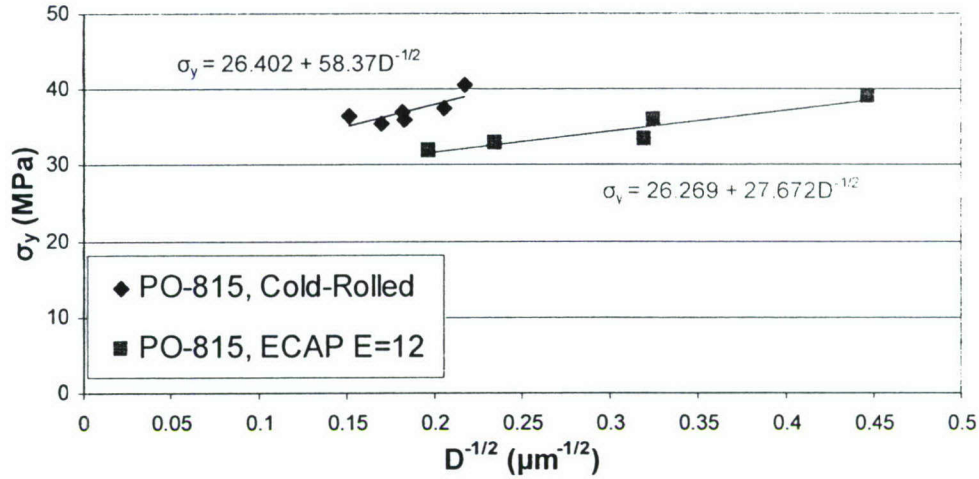

Figure 4: Hall-Petch plot for commercial purity aluminum with grain sizes and strengths produced by different processing histories.

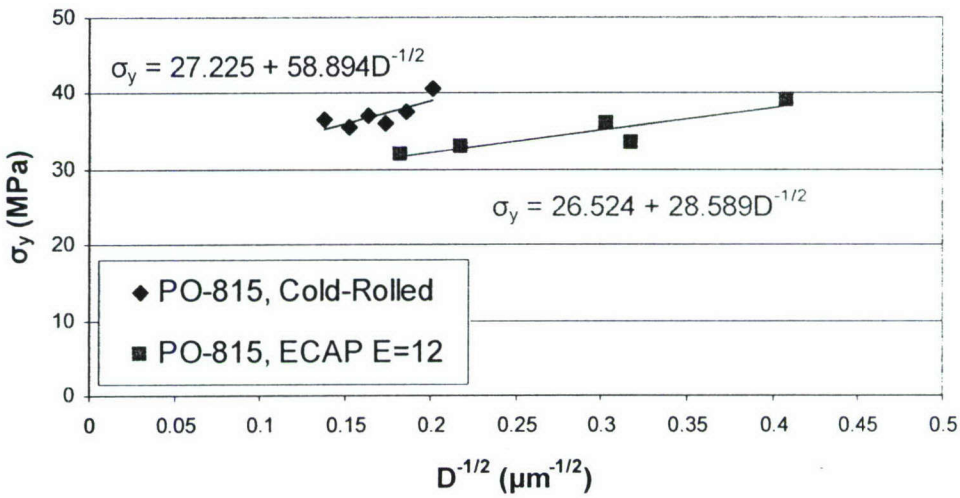

Figure 5. Data displayed in Figure 4 with only HABG being considered and LAGB ignored.

One possible source of the discrepancies in the Hall-Petch data reported in literature may be the presents of low energy-low mobility LAGB. Traditional microscopy techniques are unable to distinguish between high and low angle grain boundaries, and arguably worse, may only partially detect LAGB. This can greatly affect the reported grain size and associated yield strength of a material. The grain size and texture measurements collected in this study were performed using EBSD which allows for accurate orientation and misorientation data with 2-D spatial information. This allows for unambiguous identification of grain boundary misorientation. The data set shown in Figure 4 represents all continuous boundaries with a misorentation of greater than 3° (the angle in an angle-axes pair). If only HAGB (boundaries of 15° or greater) are considered the data sets become translated and compressed as shown in Figure 5. This produces non-trivial change in the data but it is arguable if the deviation between the two data sets is significant.

The texture correction was preformed by dividing the yield strengths by the global Taylor factors for each sample. The global Taylor factor were calculated using texture measurement data collected using EBSD and procedures developed previously in our research group [14]. When the Hall-Petch plots were corrected for texture the deviation in strength between the two processing conditions is greatly reduced, as shown in Figure 6. This strongly supports the hypothesis that texture is partially responsible for the variation in Hall-Petch data reported by different investigators for similar alloys.

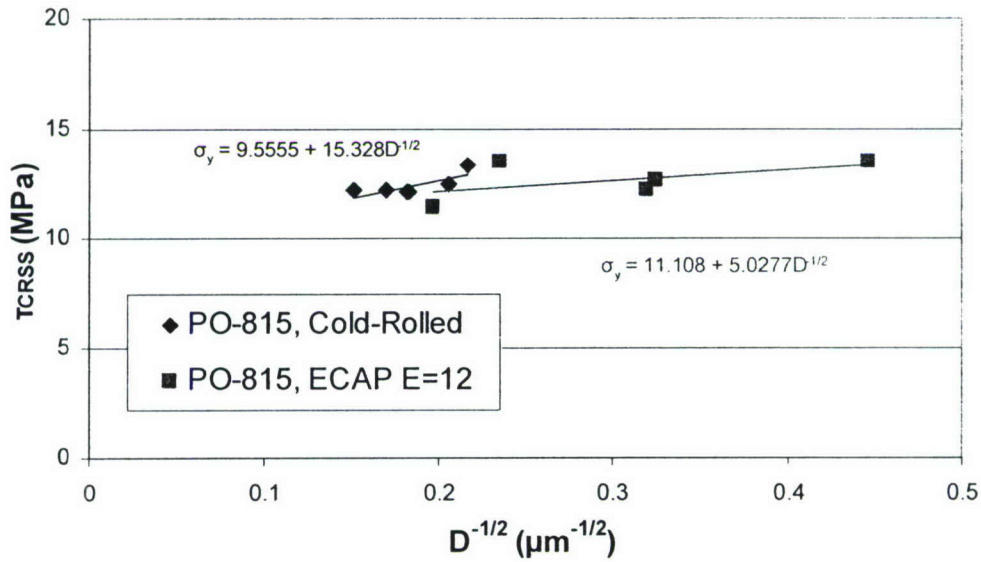

Figure 6. Data displayed in Figure 4 after being corrected for the effect of global crystallographic texture on strength.

It is indisputable that processing history plays a significant roll in the Hall-Petch relationship. The deviation in the data as a result of the history can be partially accounted for by correcting for global texture and being aware of LAGB. Due to the relatively isotropic nature of aluminum the texture effect may be more pronounced in other alloy systems. It should also be noted that depending on the material of interest the Fraction of LAGB can be as high as 48% [15, 16], compared to random value of 2-3%.

Evaluation of strain hardening as a viable processing route to produce aluminum alloys with improved combinations of yield strength and fracture toughness: A 2xxx series aluminum alloy that both effectively precipitation hardens and strain hardens was selected so that the effect of each strengthening mechanism on the mechanical performance and failure mode of the material could be investigated. The studies were aimed at answering the following questions: 1) Can Al alloys with superior or comparable strengths as traditional precipitation hardened alloys be produced without grain boundary precipitates which are known to embrittle the structure? 2) Will a strain hardened Al alloy still fail by grain boundary ductile fracture (GBDF)? 3) What is the effect of the strain hardening rate of the as-processed material on its fracture toughness?

In order to answer the questions posed above, alloy 2124 (Composition 4.5 wt% Cu, 1.5 wt% Mg, 0.5 wt% Mn) was peak aged (T6 condition) to produce the highest possible yield strength achievable by precipitation hardening in this alloy. Using the Hollomon-Stumpf and Hollomon-Ludwik equations it was estimated that a strain of 0.18 would produce an equivalent yield strength. The full details of the experimental procedure are described in [17, 18] Due to the potency of strain hardening in the 2xxx series alloys, the cold rolling operation produced a 14% higher yield strength then expected, as shown in Figure 7.

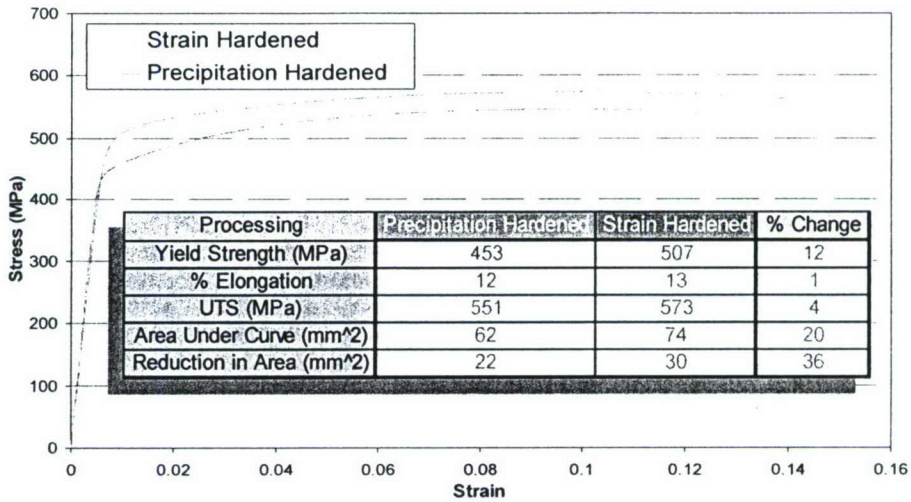

Processing	Precipitation Hardened	Strain Hardened	% Change
Yield Strength (MPa)	453	507	12
% Elongation	12	13	1
UTS (MPa)	551	573	4
Area Under Curve (mm^2)	62	74	20
Reduction in Area (mm^2)	22	30	36

Figure 7. Representative engineering stress-strain plot for alloy 2124 in both the strain hardened (to $\varepsilon = 0.18$) and precipitation hardened (T6-temper) conditions with the average test values in tabular form.

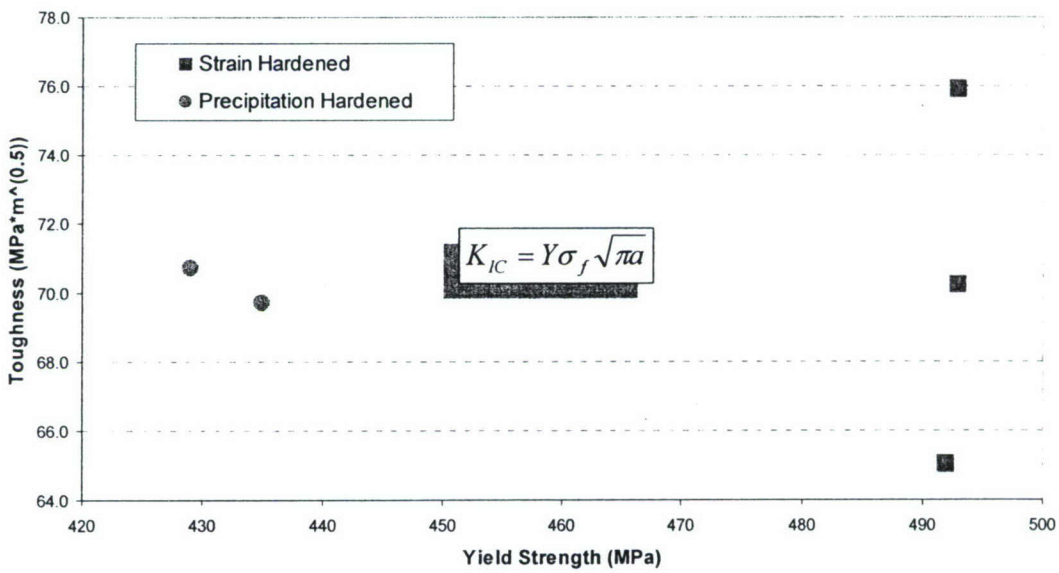

Figure 8. Toughness plotted against yield strength for alloy 2124 in the peak aged condition (12h at 190°C) and strain hardened by cold rolling (CR) to $\varepsilon = 0.18$. Note that the axis do not go through the origin.

The toughness of the samples was then measured use single-edge-notched bend (SENB) specimen loaded in three-point bending according to ASTM E 1820. The sample thicknesses were 24mm. Even this thickness did not provide plane-strain conditions. Complete experimental details can be found in [17, 18]. The apparent fracture toughness of the peak aged (PA) samples showed a reasonable deviation while that of the cold rolled (CR) was significantly more, as shown in Figure 8. The scatter in the strain hardened samples is a result of a combination of material defects and fatigue crack length. Examination of the fractured surface of the strain hardened sample that produced the erroneously low toughness value revealed an atypical surface topography, as shown in Figure 9. Energy dispersive spectroscopy (EDS) as well as further microscopy revealed the presence of oxide inclusions. These large oxide inclusions degraded the toughness of the sample producing a datum point with a value much lower than the actual value. The highest apparent toughness value in Figure 8 corresponds to a sample in which the fatigue crack barely reached the base of the chevron notch. This may have resulted in producing a higher toughness value than if the fatigue crack had been longer. The final remaining datum point, intermediate value for the strain hardened material, was free of large oxide inclusions and satisfied all fatigue crack criteria. This value is believed to be repressive of the strain hardened materials apparent toughness while at a significantly higher yield strength and equivalent to the mean apparent toughness value for the peak aged material.

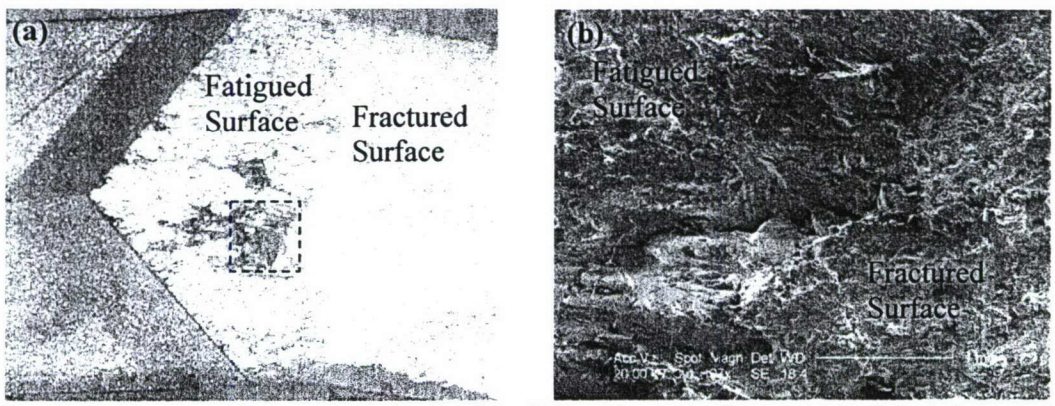

Figure 9. (a) Image of the of strain hardened sample revealing a material defect and (b) micrograph of the boxed region showing an irregularity at the fatigue interface outlined in red.

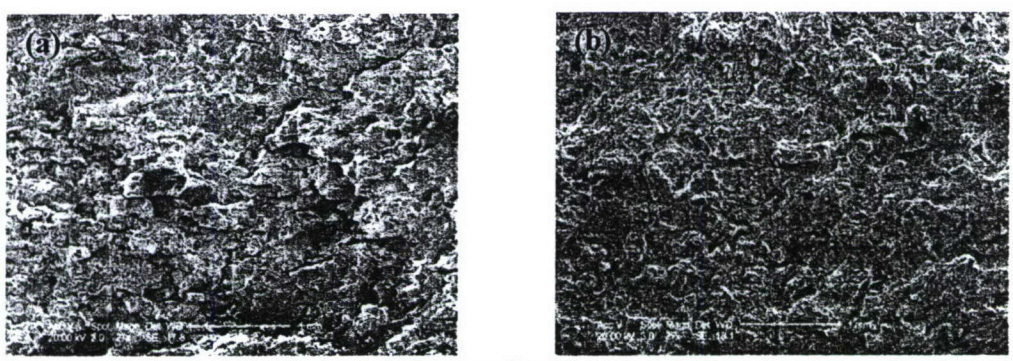

Figure 10. (a) Micrograph of the PA fractured surface exhibiting intergranular fracture and (b) of the CR fractured surface showing less cracking.

Further analyses of the fractured surfaces revealed that the precipitation strengthened samples exhibited the expected intergranular GBDF, as shown in Figure 10(a). The strain hardened samples also exhibited ductile fracture although the fracture did not follow any particular path and was transgranular, as shown in Figure 10(b). Examination of the fractured surfaces also reveals a significant difference in the spacing between dimples due to the closely spaced grain boundary precipitates acting as the initiation points for microvoids in the artificially aged material and the much wider and randomly spaced constituents acting as initiation points in the strain hardened material. It is believed that the transgranular fracture mode will provide better resistance to crack extension due to the lack of an inherently weak path to follow as in the case of GBDF.

Specimen in each processing condition were also subjected to simple compression so that the strain hardening rates could be determined. What was revealed was that even after a rolling strain of 0.18 the cold worked material still showed a higher strain hardening rate then the aged material, as shown in Figure 11. It may be possible that a higher strain hardening rate corresponds to more energy being expended in the plastic zone during fracture resulting in a higher toughness.

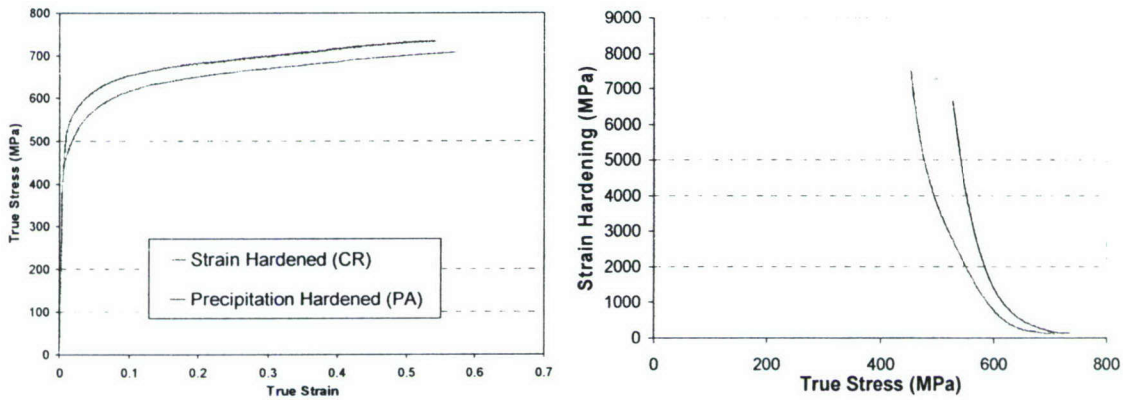

Figure 11. (a) True stress plotted against true strain of alloy 2124 in simple compression and (b) the corresponding strain hardening rate data.

2.2 Modeling Work and Accomplishments.

Prediction of Microstructure Evolution Using Crystal Plasticity Finite Element Models: In this part of our work, we have focused on the development of crystal plasticity models for the prediction of texture in ECAP samples. These models explored included the simple Taylor-type models [19] and the more sophisticated finite element models [refs]. Figure 12 shows a micromechanical finite element model of a representative volume element of a material subjected to forward and reverse shear to simulate Route C during ECAP. In this model, a crystal plasticity constitutive model [20] has been incorporated at each integration point. Furthermore, groups of eight elements in the finite element mesh are assumed to represent a grain, and are assigned a different initial crystal lattice orientation (these are selected randomly from a measured texture in the sample). The model has a total of 9600 hexagonal elements, and therefore 1200 different grain orientations. The experimental measurements were conducted by Dr. Saiyi Li and co-workers from Los Alamos National Laboratory.

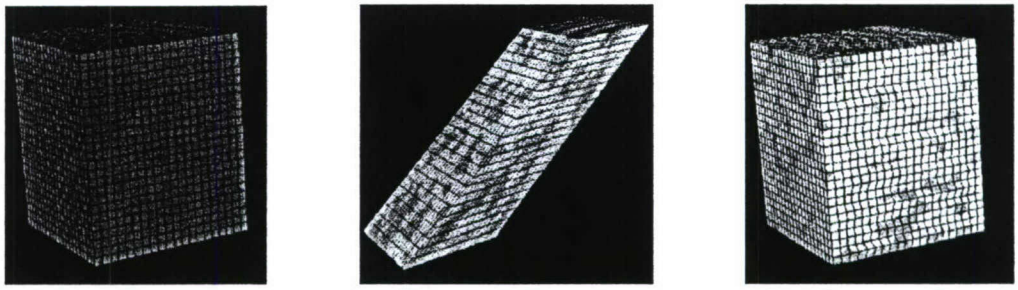

Initial Geometry **Forward Shearing** **After Reverse Shearing**

Figure 12: Initial and deformed meshes from the crystal plasticity based finite element simulations of a polycrystal representative volume element subjected to two ECAP passes by Route C.

The simulations revealed that there is a strong remnant texture in the sample after two passes by Route C. Although, the retained texture predicted by the micromechanical finite element models are in much better agreement with the experimental measurements compared to any of the previously reported modeling efforts (including predictions from Taylor model and self-consistent visco-plastic models), they are still significantly weaker in the intensity of the retained texture components compared to those measured experimentally. We strongly believe that this is because of the simplification made in the idealization of the deformation mode experienced in ECAP as simple shear.

We developed a new approach to modeling crystallographic texture evolution in ECAP. In this new approach a representative volume element of the polycrystal was subjected to boundary conditions that simulated the approximate deformation history experienced by different regions of the sample (at different through-thickness depths) in both Route A and Route C processing (see Figs. 13 and 14). Our goal was to capture the influence of the complex interactions that ensue among the constituent individual crystals of a polycrystal in controlling the texture evolution in the sample, while capturing the boundary conditions inherent to ECAE deformation. The predictions from the proposed approach were compared against previously reported experimental measurements in ECAE of copper. It was observed that the proposed approach provides significantly better agreement with the measurements when compared against any of the previously reported model predictions. Further details are provided in [21].

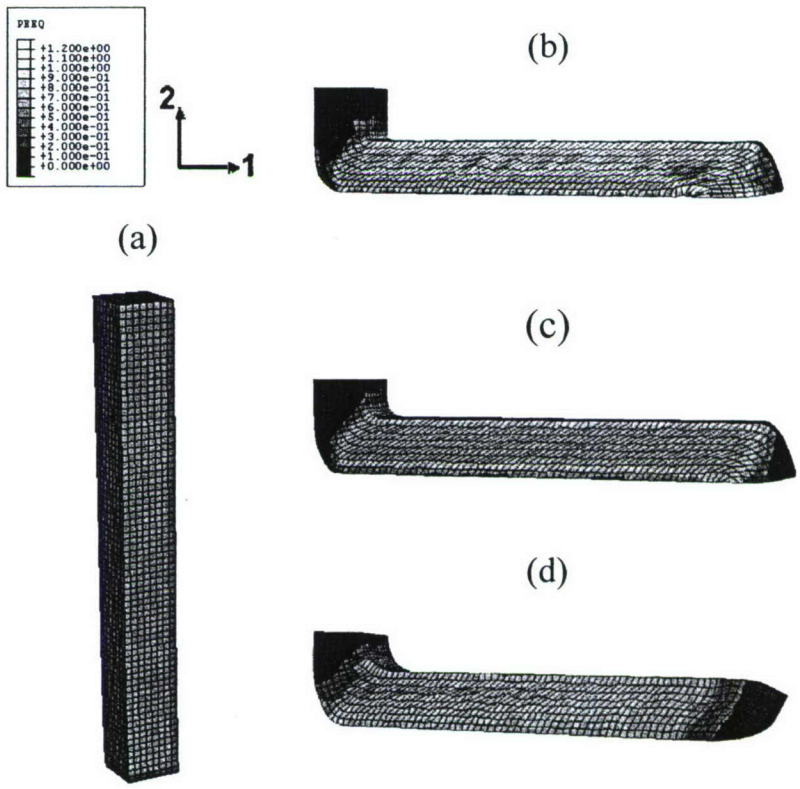

Figure 13. The finite element mesh used in the. (a) Initially undeformed mesh. (b) The deformed mesh corresponding to the upper streamline at 10% of the die thickness from the top. (c) The deformed mesh corresponding to the middle streamline at 50% of the die thickness from the top. (d) The deformed mesh corresponding to the lower streamline at 90% of the die thickness from the top. The contours shown are for the equivalent plastic strain.

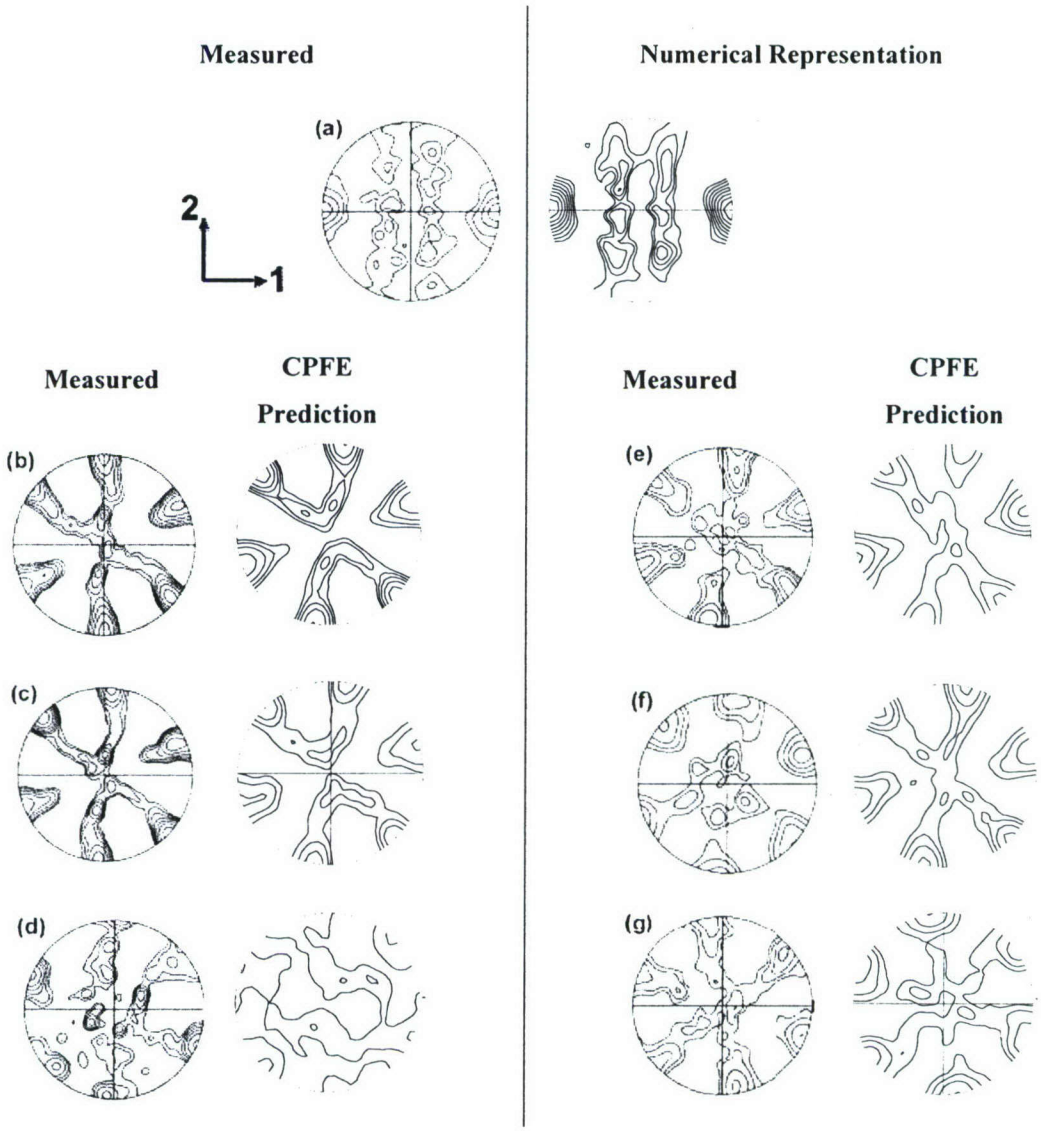

Figure 14. (a) (111) pole figures measured by OIM for Cu samples before ECAE and its numerical representation using a discrete set of representative Euler angles. Measured and predicted textures in the ECAPed samples at different locations after one and two passes of Route C; (b) top of the billet after 1 pass; (c) middle of the billet after 1 pass; (d) bottom of the billet after 1 pass; (e) top of the billet after 2 passes of Route C; (f) middle of the billet after two passes of Route C; (g) bottom of the billet after 2 passes of Route C. Contours from experiments: 1/1.4/2/2.8/4/5.6/8/11. Contours from model: 1/1.2/1.4/1.7/2.1/2.5/4.9.

3. Project Summary

1) It has been shown that deformation processing of high solute Al alloys can be carried out to higher strains before strain localization occurs if mechanical stress relieving is done prior to processing.
2) Strengths unobtainable through precipitation hardening can readily be achieved by strain hardening, as show in Figure 2&3 and Table1.
3) The effect of natural aging on strain hardening has been investigated and found to be a significant factor in the rate at which the flow stress increases with increasing plastic strain, as shown in Figure 1.
4) Strain hardened Al alloys are more ductile and exhibit higher strain hardening rates then precipitation hardened alloys at equivalent strengths and that strain hardening is a viable processing route for improving toughness, as shown in Figure 7, 8, & 11.
5) The Hall-Petch relationship is sensitive to deformation history and crystallographic texture, and can be partially corrected for each, as shown in Figures 4, 5, & 6.
6) The post-processed strain hardened material still exhibited a higher strain hardening rate than the strain free artificially aged material (T6-temper), as shown in Figure 11.
7) The expected intergranular GBDF was prevalent in the precipitation hardened alloy while transgranular fracture was observed in the strain hardened alloy (Figure 10).
8) Micromechanical finite element models have been developed to successfully simulate texture evolution in Route A and Route C ECAP.

4. Acknowledgment/Disclaimer

This work was sponsored by the Air Force Office of Scientific Research, USAF, under grant/contract number FA9550-04-1-0018. The views and conclusions contained herein are those of the authors and should not be interpreted as necessarily representing the official policies or endorsements, either expressed or implied, of the Air Force Office of Scientific Research or the U.S. Government.

5. References

1. R.E Sanders, S.F.Baumann and H.C.Stumpf 1989 in Aluminum Alloys - Contemporary Research and Applications Treatise on Materials Science and Technology 31. Eds. A.K. Vasudevan and R.D. Doherty. Academic Press. p65.
2. R.D.Doherty and J.McBride 1993 In Aluminum Alloys for Packaging Eds. J.G.Morris, H.D. Merchant, E.J. Westerman and P.L. Morris, TMS-AIME Warrendale PA. 15086, pp 347-368.
3. R.D. Doherty and S.F. Baumann 1993 In Aluminum Alloys for Packaging Eds. J.G. Morris, H.D. Merchant, E.J. Westerman and P.L. Morris, TMS-AIME Warrendale PA. 15086, pp 369-391
4. R.Z. Valiev, N.A. Krasilnikov and N.K. Tsenev, Plastic deformation of alloys with submicron-grained structure, 1991 Mater. Sci. & Eng. A137 35.
5. E.M.Shaji, S.R.Kalidindi, R.D.Doherty and A.S.Sedmak, Fracture properties of multiphase alloy MP35N, Mater. Sci. and Engr. 2003 A340 163-169
6. A.K. Vasudevan and R.D. Doherty, Overview #58, Grain boundary ductile fracture in precipitation hardened aluminum alloys. Acta Metall., 35 1193-1219.
7. C. J. Hovanec and R. D. Doherty, 2005 TMS International Conference on Solid-Solid Phase Transformations in Inorganic Materials proceedings.

8. C. J. Hovanec and R. D. Doherty , "Deformation of High Solute Aluminum Alloys and the Inhibition of GP Zone Formation". Publication pending.
9. D. Turnbull, H.S. Rosenbaum, and H. N. Treaftis, *Act Metall.* 8 (1960) 277
10. C. J. Hovanec, R. D. Doherty, and S.R. Kalidindi, "Solute Enhanced Strain Hardening of Aluminum Alloys". Publication pending.
11. C. Hovanec, R. Doherty, B. Kulesza, "Low Angle Grain Boundaries and their effect on incubation time of Abnormal Grain Coarsening", Third International Conference on Recrystallization and Grain Growth (2007).
12. R. J. VanderMeulen, Drexel University Thesis (2007)
13. C. J. Hovanec, R. J. VanderMeulen, and R. D. Doherty, "The Influence of Deformation History and Texture on the Hall-Petch Relationship" Third International Conference on Recrystallization and Grain Growth. (2007)
14. S. R. Kalidindi, C. A. Bronkhorst and L. Anand, "Crystallographic Texture Evolution During Bulk Deformation Processing of FCC Metals", *Journal of the Mechanics and Physics of Solids*, **40**, pp. 537-569, 1992.
15. C. J. Hovanec and R. D. Doherty, "Role of Frequency of Low Angle Grain Boundaries in Accelerating the Onset of Abnormal Grain Coarsening", Third International Conference on Recrystallization and Grain Growth. (2007)
16. C. J. Hovanec and R. D. Doherty, "Role of Frequency of Low Angle Grain Boundaries in Accelerating the Onset of Abnormal Grain Coarsening", Paper pending.
17. C. J. Hovanec, R. D. Doherty, and S.R. Kalidindi, "Evaluation of strain hardening as a viable processing route to produce aluminum alloys with improved combinations of yield strength and fracture toughness", Paper pending.
18. C. J. Hovanec, R. D. Doherty, and S.R. Kalidindi, "The Effect of Deformation Processing on the Strength and Toughness of High Solute Aluminum Alloys" TMS Annual Meeting and Exhibition (2007).
19 S. Ferrasse, V.M Sega, S.R. Kalidindi, F. Alford., Texture Evolution during ECAE Part I. Effect of Route, Number of Passes, and Initial Texture. Materials Science and Engineering. A368 (2004) 28-40.
20 S. R. Kalidindi, C. A. Bronkhorst and L. Anand, "Crystallographic Texture Evolution During Bulk Deformation Processing of FCC Metals", Journal of the Mechanics and Physics of Solids, vol. 40, 537-569, 1992.
21 S. R. Kalidindi, B. R. Donohue, and S. Li, "Modeling Texture Evolution in Equal Channel Angular Extrusion Using Crystal Plasticity Finite Element Models", submitted to International Journal of Plasticity.

6. Personnel Supported

Christopher J. Hovanec	Graduate Student, Drexel University, Philadelphia
Brendon R. Donohue	Graduate Student, Drexel University, Philadelphia
Ryan J. VanderMeulen	MS/BS Student, Drexel University, Philadelphia
Surya R. Kalidindi	Professor, Drexel University, Philadelphia
Roger D. Doherty	Professor, Drexel University, Philadelphia

7. Publications/Presentations

"A crystal plasticity finite element analysis of cross-grain deformation heterogeneity in equal channel angular extrusion and its implications for texture evolution", S. Li, B. R. Donohue, and S. R. Kalidindi, *Materials Science and Engineering A*, doi:10.1016/j.msea.2007.06.073, 2007.

"Low Angle Grain Boundaries and their effect on incubation time of Abnormal Grain Coarsening", C. Hovanec, R. Doherty, B. Kulesza, Third International Conference on Recrystallization and Grain Growth (2007).

"2-Point Correlations in Deformed Polycrystalline Cubic Alloys", D. Stojakovic, C. Hovanec, S. Kalidindi, Third International Conference on Recrystallization and Grain Growth (2007).

"The Influence of Deformation History and Texture on the Hall-Petch Relationship", C. J. Hovanec, R. J. VanderMeulen and R. D. Doherty, Third International Conference on Recrystallization and Grain Growth (2007).

"The Effect of Equal Channel Angular Pressing (ECAP) on the Fracture Toughness of High Solute Aluminum Alloys", C. J. Hovanec, R. D. Doherty, and S. R. Kalidindi, TMS Annual meeting and exhibition (2007).

D. Stojakovic, C. Hovanec, T. Fast, D. Fullwood, S. Kalidindi: Characterization of Polycrystalline Cubic Alloys Using 2-Point Spatial Correlations, TMS Annual Meeting and Exhibition (2007).

"Role of Frequency of Low Angle Grain Boundaries in Accelerating the Onset of Abnormal Grain Coarsening", C. J. Hovanec and R. D. Doherty, TMS Annual meeting and exhibition (2007).

"Modeling Texture Evolution in Equal Channel Angular Extrusion Using Crystal Plasticity Finite Element Models", S. R. Kalidindi, B. R. Donohue, and S. Li, submitted to International Journal of Plasticity (2007).

"Micromechanical Finite Element Crystal Plasticity Models for Prediction of Crystallographic Texture and Its Gradients During Equi-Channel Angular Processing" B. R. Donohue, S. R. Kalidindi, and C. J. Hovanec, Society of Engineering Sciences (2006).

"The Effect of Equal Channel Angular Extrusion on the Mechanical Properties of Aluminum Alloys", C. Hovanec, R. Doherty, and S. Kalidindi:, TMS Materials Science and Technology Annual Meeting and Exhibition (2006).

"Strain-Path Effects on the Evolution of Microstructure and Texture during the Severe-Plastic Deformation of Aluminum", A. A. Salem, T. G. Langdon, T. R. McNelley, S. R. Kalidindi, and S. L. Semiatin, *Metallurgical and Materials Transactions A*, **37A**, pp. 2879-2891, 2006.

"Deformation of High Solute Aluminum Alloys and the Inhibition of GP Zone Formation", C. J. Hovanec and R. D. Doherty, 2005 TMS International Conference on Solid-Solid Phase Transformations in Inorganic Materials proceedings (2005).

"Role of Low Angle Grain Boundaries in Promoting Abnormal Grain Coarsening (AGC) in the Two Phase Aluminum Alloys" Christopher Hovanec, Roger Doherty, and Arnaud Lens, presented at the Third International Conference Microstructology (2005).

"A crystal plasticity finite element analysis of texture evolution in equal channel angular extrusion" Saiyi Li, Surya R. Kalidindi and Irene J. Beyerlein, accepted for publication into Materials Science and Engineering A. Also presented at the TMS annual meeting, Feb 13-17, 2005, San Francisco, CA (2005).

"Microstructure Evolution and Mechanical Properties of Severely Plastically Deformed (SPD) Aluminum Alloys" Christopher Hovanec, Roger Doherty, and Surya Kalidindi, presented at the ASM International Young Members Meeting (2005).

"The Effect of Equal Angular Channel Processing on Mechanical Properties of Aluminum Alloys" C. J. Hovanec, R. D. Doherty, S. R. Kalidindi, A. A. Salem, and S. L. Semiatin, presented at TMS Materials Science & Technology Conference (2005).

"Abnormal Grain Coarsening and its Possible Relationship with Particle Limited Normal Grain Coarsening", R. Doherty, C. Hovanec, and A. Lens, Second International Conference on Recrystallization and Grain Growth (2004).

"Texture evolution during equal channel angular extrusion. Part I. Effect of route, number of passes and initial texture", S. Ferrasse, V.M. Segal, S. R. Kalidindi, F. Alford, Materials Science and Engineering, 2004, Vol. A368, pp. 28–40

Awards Received

Christopher Hovanec, Outstanding Young Scientist Award at the Third International Conference of Recrystallization and Grain Growth– awarded 2007.
Christopher Hovanec, GAANN Fellow – awarded 2007.
Christopher Hovanec, ASM International Best Poster Award – awarded 2007.
Christopher Hovanec, ASM International Liberty Bell Chapter Young Member of the Year – awarded 2007.
Ryan VanderMeulen, Dean's scholar at Drexel University – awarded 2007
Brendon Donohue, GAANN Fellow – awarded 2007.
Christopher Hovanec, Koerner Fellow – awarded 2006.
Christopher Hovanec, H. H. Harris Foundation Scholarship– awarded 2004, 05, 06.
Ryan VanderMeulen, Inductee in the Tau Beta Pi engineering honor society – awarded 2006
Christopher Hovanec, GAANN Fellow – awarded 2005.
Christopher Hovanec, Graduate Teaching Award – awarded 2005.
Christopher Hovanec, 1st place in the Drexel University Research Day Poster Competition – awarded 2005.

Transitions

None